MIT Libraries | DSpace@MIT

MIT Open Access Articles

Ena/VASP Is Required for Neuritogenesis in the Developing Cortex

Massachusetts Institute of Technology

Ena/VASP Is Required for Neuritogenesis in the Developing Cortex

Adam V. Kwiatkowski,[1,5,6] Douglas A. Rubinson,[1,5] Erik W. Dent,[1,7] J. Edward van Veen,[1] Jonathan D. Leslie,[1] Jiangyang Zhang,[2] Leslie M. Mebane,[1] Ulrike Philippar,[1] Elaine M. Pinheiro,[1] Aurora A. Burds,[1] Roderick T. Bronson,[3] Susumu Mori,[2] Reinhard Fässler,[4] and Frank B. Gertler[1,*]

[1]Center for Cancer Research, Massachusetts Institute of Technology, Cambridge, MA 02139, USA
[2]Department of Radiology, Division of Nuclear Magnetic Resonance Research, Johns Hopkins University School of Medicine, Baltimore, MD 2120, USA
[3]Department of Biomedical Sciences, Tufts University School of Veterinary Medicine, North Grafton, MA 01536, USA
[4]Department of Molecular Medicine, Max-Planck Institute of Biochemistry, Am Klopferspitz 18, 82152 Martinsried, Germany
[5]These authors contributed equally to this work.
[6]Present address: Department of Biological Sciences, Stanford University, Stanford, CA 94305, USA.
[7]Present address: Department of Anatomy, University of Wisconsin, Madison, WI 53706, USA.
*Correspondence: fgertler@mit.edu
DOI 10.1016/j.neuron.2007.09.008

SUMMARY

Mammalian cortical development involves neuronal migration and neuritogenesis; this latter process forms the structural precursors to axons and dendrites. Elucidating the pathways that regulate the cytoskeleton to drive these processes is fundamental to our understanding of cortical development. Here we show that loss of all three murine Ena/VASP proteins, a family of actin regulatory proteins, causes neuronal ectopias, alters intralayer positioning in the cortical plate, and, surprisingly, blocks axon fiber tract formation during corticogenesis. Cortical fiber tract defects in the absence of Ena/VASP arise from a failure in neurite initiation, a prerequisite for axon formation. Neurite initiation defects in Ena/VASP-deficient neurons are preceded by a failure to form bundled actin filaments and filopodia. These findings provide insight into the regulation of neurite formation and the role of the actin cytoskeleton during cortical development.

INTRODUCTION

The intricate structure of the mammalian forebrain is formed through orchestrated movement of neurons and their processes. Neurons born in internal germinal regions migrate tangentially and radially to occupy more superficial layers and establish the architectonic framework of the forebrain (Marin and Rubenstein, 2003). Migrating neurons possess leading and trailing processes morphologically similar to growth cones (Lambert de Rouvroit and Goffinet, 2001) that are postulated to develop into dendrites (Hand et al., 2005; Hatten, 2002; Olson et al., 2006) and axons (Noctor et al., 2004; Tsai et al., 2005),

respectively. Subsequent guided outgrowth of axons forms the fiber tracts essential for cortical function (Sur and Rubenstein, 2005). Similar guidance molecules are used by both the leading processes of migrating neurons and axonal growth cones, suggesting there could be functional similarities between these two structures (Lambert de Rouvroit and Goffinet, 2001; Song and Poo, 2001; Yee et al., 1999). Little is known, however, about the mechanisms underlying the initial emergence of axons from the neuronal cell body (Luo, 2002).

Neurons are born as spherical cells, yet their biology requires a highly polarized morphology. Sprouting of neurites—cylindrical extensions tipped by growth cones that lack the defining features of an axon or dendrite—from spherical neurons breaks their symmetry (da Silva and Dotti, 2002). In vitro, cortical neurons form neurites after 1 day in culture, followed by rapid elongation of one neurite to form an axon (de Lima et al., 1997). In vivo, neuritogenesis is believed to occur shortly after neuronal commitment in the germinal layer; axon formation only occurs after migration has commenced (Noctor et al., 2004). It has been suggested that fundamental events in neurite formation are similar in vitro and in vivo (da Silva and Dotti, 2002); however, little evidence exists to support this, and the molecular mechanisms underlying neurite formation remain largely unknown.

Actin regulatory proteins play a key role in neuronal migration and axonal outgrowth and guidance. Ena/VASP proteins bind actin and regulate the assembly and geometry of F-actin networks by antagonizing capping proteins and bundling actin filaments (Krause et al., 2003). They are required for filopodia formation in a variety of cell types, including: *Dictyostelium* (Han et al., 2002; Schirenbeck et al., 2006), fibroblasts (Applewhite et al., 2007; Mejillano et al., 2004), and neuronal growth cones (Adler et al., 2006; Dwivedy et al., 2007; Lebrand et al., 2004). In addition, Ena/VASP proteins function downstream of attractive and repulsive axon guidance pathways (Krause et al., 2003). In mice, past work has
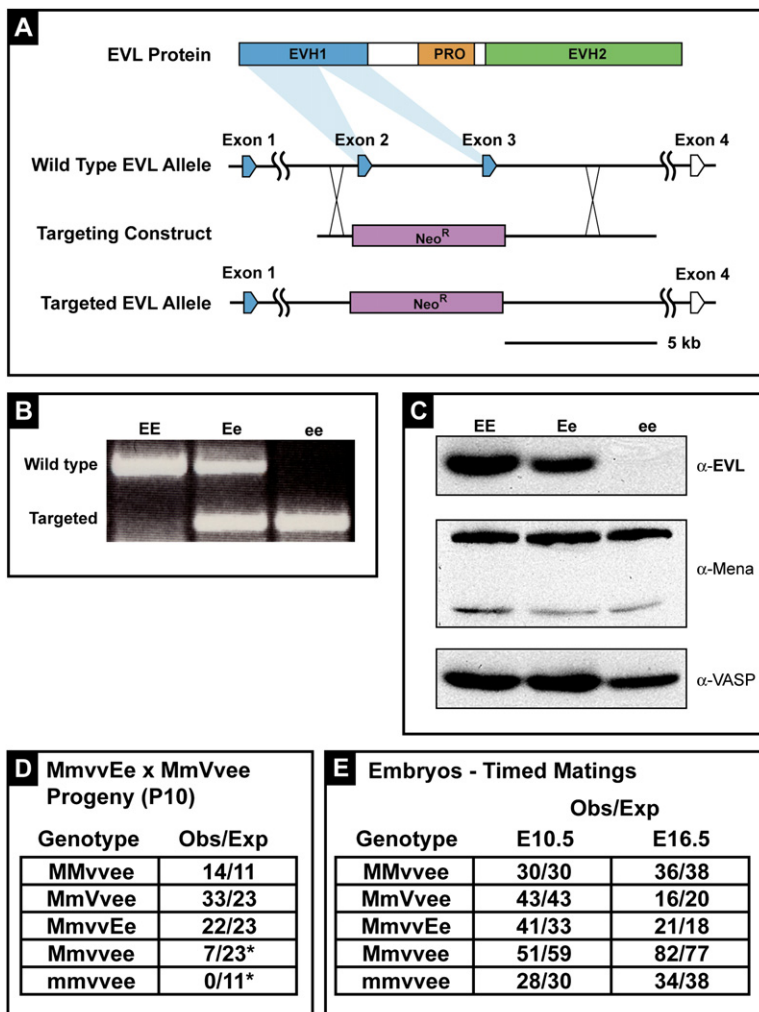
Figure 1. EVL Targeting and Recovery of Ena/VASP Mutants

(A) Targeting vector containing a neomycin resistance cassette flanked by genomic DNA from introns 1 and 3 of the EVL locus. Homologous recombination deleted exons 2 and 3 of EVL, removing most of the N-terminal EVH1 domain and producing a downstream frameshift.

(B) PCR genotyping of tail samples from offspring of an EVL heterozygous intercross (Ee × Ee). Wild-type and targeted alleles are noted.

(C) Western blot analysis of extracts from wild-type (EE), heterozygous (Ee), and homozygous mutant (ee) adult mouse brains. Equal amounts of total protein were loaded and analyzed for levels of EVL, Mena, and VASP. No EVL protein was detected in ee lysates, indicating that the targeted allele eliminated EVL expression. No measurable difference in Mena and VASP expression was observed in ee lysates.

(D) MmvvEe by MmVvee crosses yielded viable MMvvee, MmVvEe, MmvvEe, and Mmvvee animals at P10. Viable mmvvee mutants were never observed at P10. Asterisks indicate a statistically significant reduction as determined by χ^2 analysis in a given population (p < 0.05).

(E) Embryos were collected at E10.5 and E16.5 from timed matings and genotyped. Near-expected number of mmvvee embryos were collected at both stages, suggesting that Ena/VASP proteins were not required for early developmental events and that mmvvee mutants died at or near birth.

implicated Ena/VASP proteins in midline crossing of axons and neuronal migration in the forebrain (Goh et al., 2002; Lanier et al., 1999; Menzies et al., 2004). However, the presence of three vertebrate proteins with similar functions (Loureiro et al., 2002) and overlapping expression patterns in the neocortex (Goh et al., 2002; Lanier et al., 1999) precluded complete analysis of Ena/VASP function during cortical development.

Here we report the first examination of cortical development in the complete absence of Ena/VASP. We show that loss of Ena/VASP causes two defects in neuronal migration during corticogenesis: a defect in cortical positioning and a non-cell-autonomous defect in pial membrane integrity that causes neuronal ectopias. Unexpectedly, we find that loss of Ena/VASP blocks axon fiber tract formation in the cortex, and we demonstrate that this defect results from the failure of cortical neurons to produce neurites. We offer further evidence to suggest that the defect in neurite formation results from the inability of Ena/VASP-deficient neurons to make filopodia. Finally, we demonstrate that neurite formation can be uncoupled

from neuronal migration. Our results define new roles for Ena/VASP in corticogenesis and offer new insights into the relationship between axon formation and neuronal migration.

RESULTS

Generation of Ena/VASP Null Mutants

Vertebrates possess three Ena/VASP proteins: Mena (mammalian enabled), VASP (vasodilator stimulated phosphoprotein), and EVL (Ena-VASP like) (Gertler et al., 1996). Construction and analysis of Mena and VASP protein null mutants and Mena/VASP double mutants in mice have been reported (Aszodi et al., 1999; Lanier et al., 1999; Menzies et al., 2004). We targeted the remaining Ena/VASP locus, *EVL* (Figure 1A). Animals homozygous for the targeted EVL allele (ee) produced no detectable EVL by western blot (Figures 1B and 1C). Mutant ee mice were viable; gross morphological and histological analysis of ee mice revealed no obvious defects (data not shown).

Mutant ee mice were crossed to existing Mena (Lanier et al., 1999) and VASP (Aszodi et al., 1999) mutant lines, and viable Ena/VASP triple mutant combinations intercrossed. Results from these crosses are shown in Figure 1D. Triple null (mmvvee) progeny were never observed at P10 (0 of 11 expected). Interestingly, a single allele of Mena was sufficient to produce viable and fertile mice, albeit at a significantly reduced frequency. In contrast, neither two alleles of EVL (mmvvEE; Menzies et al., 2004) nor two alleles of VASP (mmVVee, this study, data not shown) were sufficient for viability. Thus, Mena was the most critical Ena/VASP protein for development and survival, though whether this reflected a unique expression pattern, level, and/or indispensable function of Mena remains unclear. Mice possessing one allele of Mena and a second Ena/VASP allele (MMvvee, MmVvee, MmvvEe) were viable with no obvious defects in brain morphology (data not shown) and were used as controls for histological and cell biological experiments.

To determine how far mmvvee mutants progressed through development, timed matings between triple mutant combinations were established and embryos isolated at E10.5 and E16.5. Interestingly, 93% (28/30) of expected mmvvee embryos were collected at E10.5, and 89% (34/38) were recovered at E16.5 (Figure 1E). Therefore, Ena/VASP proteins were not required for cell migration during early developmental events such as gastrulation. Lethality of mmvvee mice occurred between E16.5 and P0 and resulted from a number of defects, including intraamniotic hemorrhage, hydrops fetalis, and frequent exencephaly. Extraneuronal phenotypes will be described elsewhere (Furman et al., 2007); here we focus on phenotypes affecting cortical development.

Loss of Ena/VASP Causes Cobblestone Cortex

The majority of mmvvee embryos (86%) were exencephalic, precluding analysis of brain development. Since nonexencephalic mmvvee embryos were limiting, we employed MRI to assay for structural lesions noninvasively. Diffusion-weighted MRI revealed hydrocephalus ex vacuo in the mmvvee embryo (Figure 2B, compare to 2A). Hematoxylin and eosin (H&E) staining of brain sections confirmed defects in ventricle size and total brain matter in mmvvee brains (see Figure S1 in the Supplemental Data available with this article online) with no evidence of increased apoptosis, confirmed by TUNEL assay (data not shown).

Diffusion tensor microimaging (μDTI) permits visualization of brain organization, including cortical layering and individual fiber tracts (Zhang et al., 2005). Strikingly, μDTI revealed an additional cortical layer outside the cortical plate (CP) in the mmvvee cortex (Figure 2D, blue arrow, compare to control in 2C). Subsequent histological analysis revealed that this additional cortical layer corresponded to neuronal ectopias (Figure 2E, black arrows; Figure S1), hallmarks of the human congenital malformation cobblestone cortex (Olson and Walsh, 2002). Ectopias were observed in 5 of 7 nonexencephalic mmvvee

brains studied, but never in brains from embryos expressing one or more Ena/VASP allele. Ectopias appeared as stochastic and infrequent (0–10 per brain) intrusions beyond the pial membrane (PM) with marked tangential spread of ectopic neurons within the subarachnoid space (Figures 2E and 2I; Figure S1). β3-tubulin staining confirmed that ectopias were comprised largely of differentiated neurons (Figure 2F).

Known human syndromes—Fukuyama congenital muscular dystrophy, muscle-eye-brain disease, Walker-Warburg syndrome—and mouse models of cobblestone cortex are associated with defects in PM formation and integrity (Olson and Walsh, 2002). Laminin is the predominant extracellular matrix (ECM) protein of the PM and is produced and organized by meningeal fibroblasts (Miner and Yurchenco, 2004; Sievers et al., 1994). Failure of meningeal fibroblasts to produce and organize laminin properly has been linked to ectopia formation in mouse models of cobblestone cortex (Beggs et al., 2003). We cultured meningeal fibroblasts from mmvvee mutants and found that, similar to controls (Figure 2G), mmvvee cells secreted and organized laminin into fibrillar structures (Figure 2H). Consistent with this, laminin staining in mmvvee brains lacking ectopias appeared similar to controls (Figures 4G and 4H). Although breaks in the laminin matrix were observed at sites of ectopic neuron exit, laminin staining surrounding ectopias appeared normal (Figures 2I and 2L).

Radial glia processes span the cortex and their endfeet contact with, and promote organization of, the basement membrane (Halfter et al., 2002). Disruptions in endfeet attachment to the PM are observed in multiple mouse models of cobblestone cortex (Beggs et al., 2003; Halfter et al., 2002; Niewmierzycka et al., 2005). To assess radial glia morphology, we stained control and mmvvee cortices for the radial glia marker nestin. Well-organized, nestin-positive glia were observed making contact with the PM in control cortices (Figure 2J). Along the PM, the tufted endfeet of radial glia were conspicuous (Figure 2J, white arrow and inset). In mmvvee cortices lacking ectopias, nestin staining was reduced in areas along the PM (Figure 2K, white arrow and inset), reflecting a possible defect in endfoot formation and/or attachment. Interestingly, aberrant extension of radial processes into ectopic growths was noted (Figure 2L, white arrows). We speculate that loss of Ena/VASP disrupts radial glia endfoot morphology and/or function, compromising barrier integrity and permitting ectopia formation.

Ena/VASP Regulates Cortical Positioning

The extent of neuronal tangential spread within mmvvee ectopias is distinct from other models of cobblestone cortex and may represent a defect in neuronal migration. During corticogenesis, neurons born in the ventricular zone (VZ) migrate radially outward to form the CP. The CP is generated with an inside-out topology, with later-born neurons migrating beyond earlier-born neurons to form the superficial layers of the cortex (Marin and Rubenstein,
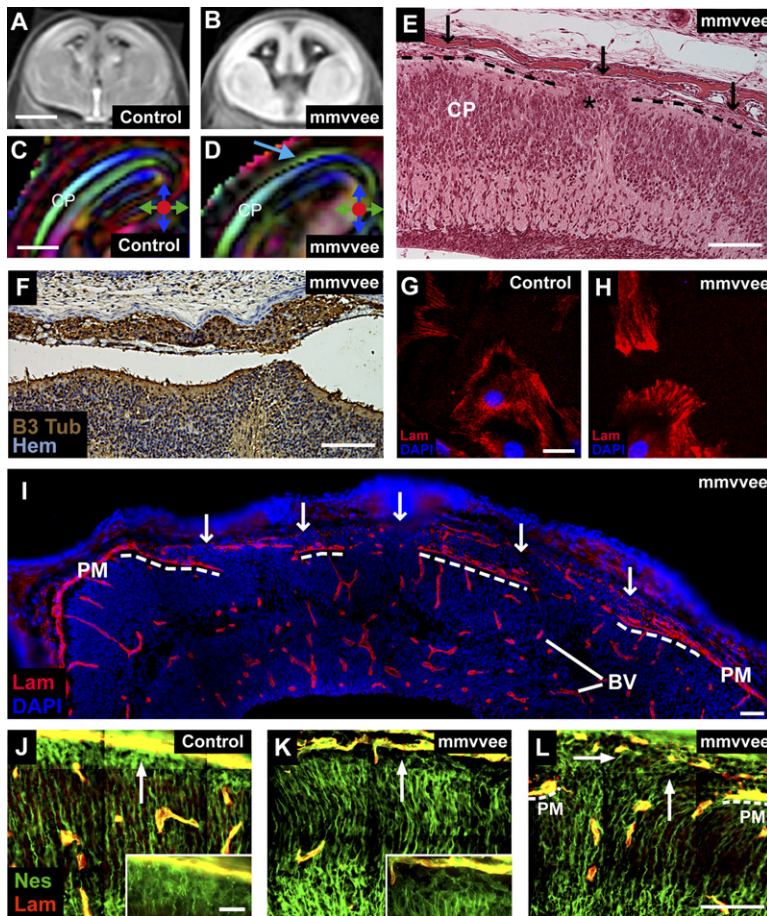
Figure 2. Loss of Ena/VASP Causes Cobblestone Cortex

(A and B) Coronal diffusion-weighted MRI of E16.5 heads. Unlike the littermate control (A), hydrocephalus was evident in the mmvvee brain (B) with enlargement of all ventricles (black regions within brain).

(C and D) µDTI of coronal sections, in which color represents the restriction of tissue water diffusion to a single plane: red is anterior-posterior, green is medial-lateral, and blue superior-inferior. Orientation is denoted by the colored orthogonal arrows. µDTI revealed an additional cortical layer (blue arrow) above the cortical plate (CP) in multiple planes of the mmvvee brain (D).

(E) H&E staining of sagittal sections (5 µm) through an E18.5 mmvvee head revealed cortical ectopias in the forebrain. Note the marked tangential spread of ectopic neurons (black arrows) beyond the initial breach (black asterisk) of the pial membrane (black dashed line). Cortical plate (CP).

(F) β3-tubulin staining (B3 Tub, brown) of sagittal sections (5 µm) from E16.5 mmvvee embryo heads confirmed that cortical ectopias were composed largely of differentiated neurons. Sections were counterstained with hematoxylin (Hem, blue).

(G and H) Meningeal fibroblasts from E14.5 control and mmvvee littermates were stained for extracellular laminin (Lam, red) and DAPI (blue). mmvvee meningeal fibroblasts (H) produced and organized laminin similar to controls (G).

(I) Laminin (Lam, red) and DAPI (blue) staining of coronal sections (10 µm) from mmvvee embryos revealed frequent breaks in the pial membrane (PM, marked with dashed white line) and multiple ectopias (white arrows). Outside of ectopias, laminin staining appeared normal. Laminin-rich blood vessels (BV) were also labeled.

(J–L) Coronal sections (10 µm) from control and mmvvee E16.5 cortices were stained with anti-nestin antibodies to label radial glia (Nes, green) and anti-laminin to label the PM (Lam, red). In controls, radial glia processes were organized in a parallel array with tufted endfeet terminating at the PM ([J], white arrow, inset). Outside of ectopias in mmvvee cortices, endfeet lacked tufts and appeared detached from the PM ([K], white arrow, inset). At ectopias, the PM (dashed white line) was disrupted in mmvvee cortices, and radial glial processes extended into ectopias ([L], white arrows). Laminin-rich blood vessels in the CP were stained in both control and mmvvee sections.

Scale bar for (A) and (B), 1 mm; for (C) and (D), 500 µm; for (E), 100 µm; for (F), 100 µm; for (G) and (H), 10 µm; for (I), 100 µm; for (J)–(L), 100 µm; insets, 25 µm.

2003). We sought to determine whether loss of Ena/VASP disrupted CP topology; however, nonexencephalic mmvvee embryos were severely limited in number. Furthermore, neuronal ectopias in mmvvee embryos altered CP topology drastically (Figures 2E and 2I; Figure S1), making it difficult to discern a primary defect in neuronal migration. Therefore, we generated chimeric embryos composed of Ena/VASP null (mmvvee) and wild-type (WT) cells to overcome these obstacles and permit analysis of cell-autonomous defects in neuronal migration.

To construct chimeric embryos, we isolated and cultured mmvvee embryonic stem (ES) cells, and infected these cells with lentivirus expressing EGFP. Stable, EGFP-expressing (GFP+) mmvvee ES cell clones were isolated, expanded, and then injected into WT blastocysts (Figure 3A). Chimeric embryos were harvested from E16.5 to E18.5. As hoped, mid to high percentage chimeras

(>50% GFP+ mmvvee cells) were not exencephalic, permitting analysis of forebrain structure and composition. Gross cortical architecture appeared unperturbed in chimeric brains, with GFP+ mmvvee cells distributed broadly (Figure S2). Interestingly, neuronal ectopias were never observed in chimeric embryos, even in those in which the vast majority of cortical neurons were mmvvee in origin (Figure S2), indicating that the underlying cause of neuronal ectopia formation was likely nonautonomous.

To determine if loss of Ena/VASP affected neuronal migration and cortical layering, we stained E18.5 chimeric cortices for the layer-specific transcription factors Tbr1 (layer VI) (Hevner et al., 2001) and Foxp1 (layers III-V) (Ferland et al., 2003). For each layer marker, the distribution of WT (GFP−) and mmvvee (GFP+) nuclei was examined. Nearly all Tbr1-positive nuclei were located within a 450–500 nm thick band above the intermediate zone (IZ), the
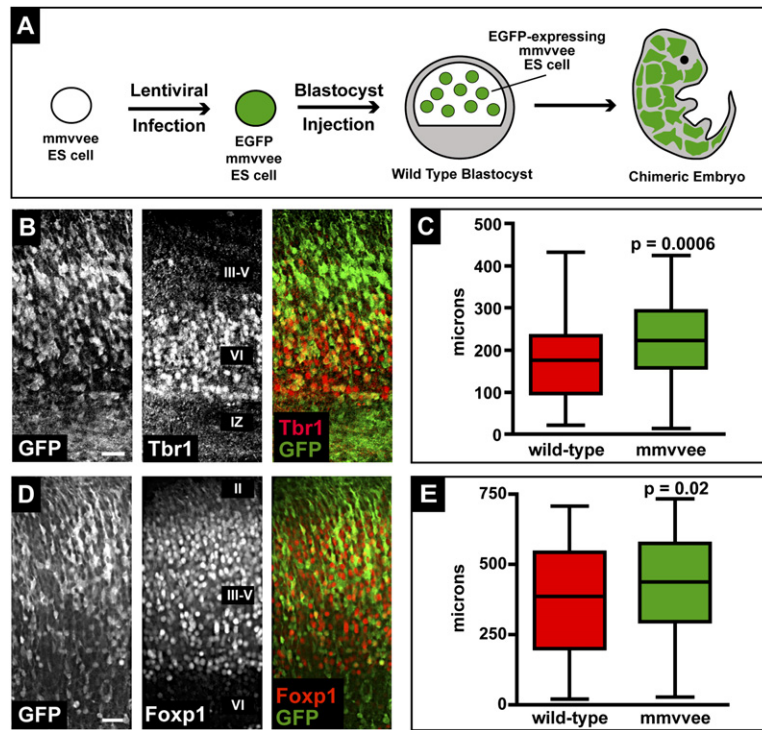
Figure 3. Ena/VASP Regulates Intralayer Cortical Positioning in Chimeric Embryos

(A) Generation of Ena/VASP-deficient chimeric embryos. mmvvee embryonic stem (ES) cells were isolated, infected with lentivirus expressing EGFP and sorted for GFP expression. GFP+ mmvvee ES cell clones were injected into wild-type (WT) blastocysts, and resulting chimeric embryos were isolated at various stages of development. Ena/VASP-deficient tissues and cells were clearly identified as GFP+.

(B and D) Coronal vibratome sections (100 μm) from a chimeric E18.5 embryo were stained for Tbr1, a marker for layer VI neurons in the CP (B), or Foxp1, a marker for layers III-V (D). GFP (green), Tbr1 or Foxp1 (red), and merged channels are shown from a representative cortical section. Images in (B) contain layers III-V, VI, and intermediate zone (IZ); images in (D) contain layers II, III-V, and VI. While no gross disruption in layer VI (B) or layers III-V (D) formation was observed in chimeric brains, GFP+ mmvvee neurons concentrated in the upper regions of layer VI and layers III-V.

(C and E) The position of WT and mmvvee (GFP+) nuclei in layer VI (Tbr1+) and layers III-V (Foxp1+) was measured. All nuclei were measured relative to the bottom of each layer/s. The results of these measurements are shown as microns from the bottom of the layer/s in a box and whisker format: the ends of the box mark the upper and lower quartiles, the horizontal line in the box is the median, and the "whiskers" outside the box extend to the highest and lowest value. Tbr1+ WT and mmvvee neurons were all contained within a 425–450 micron thick layer in the CP, as reflected by nearly identical "whisker" profiles (C). However, Tbr1+ mmvvee neurons were concentrated in the upper region of the layer compared to WT (unpaired t test, p = 0.0006). Similarly, Foxp1+ WT and mmvvee neurons were all contained within a 750 micron thick region in the CP (E). Foxp1+ WT neurons were equally distributed through this region, whereas mmvvee neurons were shifted upward slightly, but significantly (unpaired t test, p = 0.02).
Scale bar for (B) and (D), 50 μm.

expected location of layer VI (Figure 3B). Interestingly, GFP+/Tbr1+ mmvvee nuclei were shifted outward significantly within the band, occupying a more superficial region of layer IV compared to WT nuclei (Figure 3C). A similar trend was observed in Foxp1+ nuclei: GFP+ mmvvee nuclei were shifted outward significantly within, but not outside of, layers III-V (Figures 3D and 3E). Thus, while Ena/VASP was dispensable for neuronal migration and CP formation, intralayer neuronal positioning was altered.

Fiber Tract Formation Requires Ena/VASP

μDTI revealed that, in regions without ectopias, the gross architecture of the CP was preserved in the mmvvee embryo (Figures 4B and 4D) compared to the control (Figures 4A and 4C). However, the mmvvee embryo IZ lacked μDTI signal, indicating absence of organized axon tracts (Figures 4C and 4D; orange arrow points to IZ). Further μDTI analysis revealed that all cortical fiber tracts were absent in the mmvvee brain, including all major forebrain commissures and the internal capsule (IC; data not shown). Histological examination confirmed that cortical architecture, ectopias aside, was largely normal in mmvvee cortices (Figure 2E; Figure S1). However, DAPI staining revealed that the relatively cell-free IZ in mmvvee cortices was sig-

nificantly thinner than in littermate controls (Figure 4F, compare to 4E). The IZ is comprised largely of axons from migrating and established CP neurons; thus, the observed defects could result from a failure either to form or elongate axons in vivo.

To establish if loss of Ena/VASP perturbed fiber tract formation, cortical sections were stained for mid-sized neurofilament protein (NF). NF proteins are abundant intermediate filament proteins concentrated in mature axons and serve as a marker for axonal outgrowth and maturation (Elder et al., 1998; Friede and Samorajski, 1970). In controls, the NF antibody decorated mature axons in the IZ and IC (Figure 4G). In striking contrast, the IZ of mmvvee cortices was nearly devoid of NF+ axons (Figure 4H), with only a few NF+ fibers near where the IC should be found. The lack of NF labeling suggested that mature axons were not formed in mmvvee cortices, resulting in a thin and disorganized IZ and preventing cortical fiber tract assembly.

To determine if axons were formed, sections from control and mmvvee cortices were stained with an antibody to dephospho-Tau (Tau-1), a specific marker for axons in situ. In control sections, Tau-1 labeling was strongest in the axon-rich IZ (Figure 4I). Staining was also observed in the CP and subventricular zone (SVZ), where individual
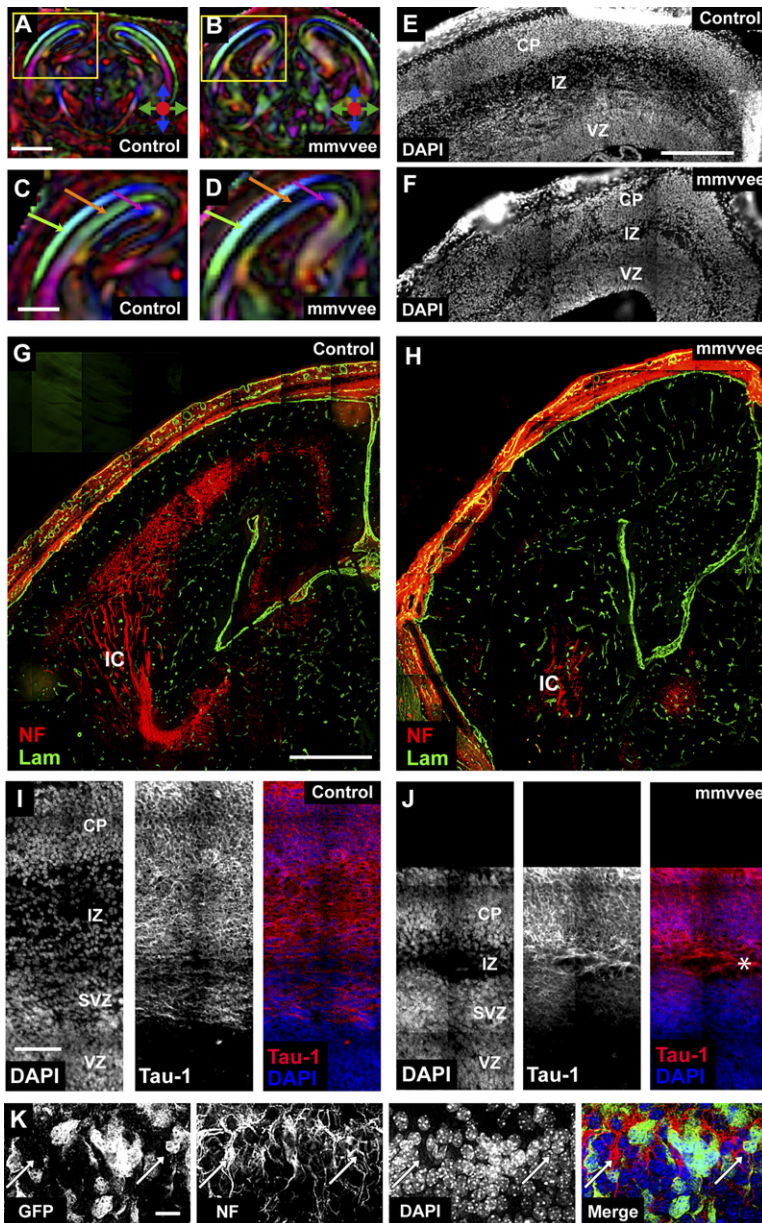
Figure 4. Ena/VASP Is Required for Axonal Outgrowth and Fiber Tract Formation in the Developing Cortex

(A–D) μDTI of coronal sections through E16.5 control (A and C) and mmvvee (B and D) brains. Tissue orientation is denoted by the colored orthogonal arrows in (A and B). Magnification of the area enclosed in the yellow box (A) revealed a well-defined cortical plate (green arrow), intermediate zone (orange arrow), and ventricular zone (purple arrow) in the control brain (C). In contrast, examination of a similar region in the mmvvee brain ([B], yellow box) revealed that the thickness and organization of the intermediate zone was markedly decreased (D).

(E and F) DAPI staining of E16.5 matched coronal sections exposed the thin cell-free intermediate zone (IZ) in mmvvee cortices (F) compared to littermate controls (E). Cortical plate (CP) and ventricular zone (VZ) thickness was similar between sections.

(G and H) Anti-neurofilament (NF) immunostaining of coronal sections (10 μm) through the heads of control and mmvvee E16.5 embryos. Labeling control sections (G) with anti-NF (red) and anti-laminin (Lam, green) revealed subcortical projections running through the IZ and into the internal capsule (IC). Strikingly, cortical fiber tracts were completely absent from mmvvee brains (H). Limited staining was observed in the IC that could represent either descending subcortical axons and/or ascending thalamocortical fibers.

(I and J) Coronal sections through similar regions of E16.5 control (I) and mmvvee (J) brains were stained for dephospo-Tau (Tau-1, red) to label axons and DAPI (blue). Individual channels and merge are shown. In controls (I), Tau-1 staining was concentrated in the axon-rich IZ and observed in the CP as well as the SVZ, where individual processes/fibers were observed. In contrast, Tau-1 staining was concentrated in the substantially thinner IZ of mmvvee cortices (J), where fibers appeared snarled and disorganized (white asterisk). Reduced staining was also noted in the SVZ.

(K) Cortical frozen sections (10 μm) from chimeric embryos at E16.5 were stained with DAPI, anti-GFP, and anti-NF. Individual channels and merge are shown. NF+ processes were only observed emanating from WT (GFP−) neurons (white arrows).

Scale bar for (A) and (B), 1 mm; for (C) and (D), 500 μm; for (E) and (F), 500 μm; for (G) and (H), 500 μm; for (I) and (J), 100 μm; for (K), 50 μm.
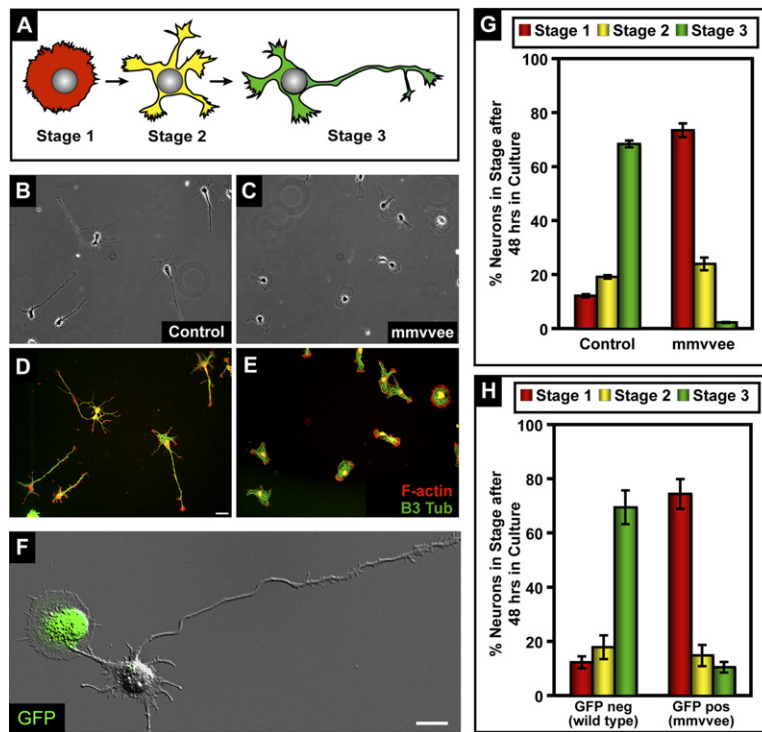
fibers were observed. In mmvvee cortices, Tau-1 staining was observed in the rudimentary IZ, where it labeled disorganized and snarled fiber-like structures (Figure 4J, white asterisk). Reduced staining was also noted in areas of the SVZ, possibly reflecting a failure of radially migrating cortical neurons to form axons. The defects in Tau-1 staining were consistent with a failure to form axons properly in the absence of Ena/VASP.

To examine axon formation at the single-cell level, we analyzed formation of NF+ processes in chimeric embryos. While NF+ axonal processes were observed in chimeric cortices, close examination revealed that they lacked GFP expression, indicating that they belonged to WT, not mmvvee, cells (Figure 4K). In contrast, neighboring GFP+ mmvvee neurons failed to extend processes in the same environment (Figure 4K).

Ena/VASP Is Required for Neurite Initiation In Vitro

The defects observed in vivo could reflect a requirement for Ena/VASP proteins in neurite initiation, axon formation,

Figure 5. Loss of Ena/VASP Inhibits Neurite Initiation in Cortical Neurons

(A) Stages of cortical neuron development in vitro. Stage 1 neurons exhibit extensive lamellipodia and filopodia-rich periphery with no processes. Stage 2 neurons possess one or more minor processes but have not yet extended an axon, while stage 3 neurons have extended a single axon.

(B–E) Cortical neurons cultured from E14.5 control and mmvvee littermates for 48 hr, fixed, and stained for F-actin (red) and β3-tubulin (B3 Tub, green). Shown are representative fields of cells imaged in phase (B and C) and fluorescence (D and E). The majority of control cortical neurons possessed a well-defined axon (B and D), whereas most mmvvee neurons lacked neurites (C and E).

(F) Cortical neurons cultured from E14.5 chimeric embryos for 48 hr and fixed. A fluorescence image overlaying a DIC image is shown to identify the GFP+ mmvvee neuron. Most GFP+ mmvvee neurons lacked neurites, whereas most wild-type (WT) neurons possessed a well-defined axon.

(G) Scoring for developmental stage after 48 hr in culture revealed that the majority (65%) of control neurons were in stage 3, while the majority (70%) of mmvvee neurons were in stage 1.

(H) Cortical neurons from chimeric embryos were scored for both GFP expression and stage development. GFP− WT neurons were predominantly in stage 3 (70%), whereas the majority (75%) of GFP+ mmvvee cortical neurons were in stage 1.

Scale bar for (B)–(E), 20 μm; for (F), 10 μm. Data shown are means ± SEMs.

and/or axon elongation. In culture, cortical neuritogenesis follows a well defined set of stages (de Lima et al., 1997). Stage 1 cortical neurons produce extensive lamellipodia and filopodia around their periphery. Stage 2 neurons possess multiple neurites, but not an established axon. Stage 3 neurons extend a single axon from one of their multiple neurites (Figure 5A). To explore a role for Ena/VASP in neuritogenesis and/or axonogenesis, we cultured cortical neurons from mmvvee brains in vitro. Representative fields of fixed cells isolated from control and mmvvee cortices are shown in phase-contrast micrographs (Figures 5B and 5C) and stained for F-actin and β3-tubulin (Figures 5D and 5E). Strikingly, after 48 hr in culture, 74% of cortical neurons from mmvvee embryos remained in stage 1, with only 2% reaching stage 3 (Figure 5G). This was in sharp contrast to control littermates, where only 10% of neurons were in stage 1, and 69% developed to stage 3 (Figure 5G). Long-term time-lapse analysis of cortical neurons in culture revealed the small fraction of mmvvee neurons that reached stage 2 all eventually progressed to stage 3 (data not shown). Thus, the defect in mmvvee cortical neurons was largely a failure to progress from stage 1 to stage 2, defined as neurite initiation or neuritogenesis. In contrast, Ena/VASP was not required for axonal polarization.

To provide a precise comparison of neuritogenesis between WT and mmvvee mutant neurons, cortical neurons from chimeric E14.5 embryos were isolated and scored for

stage development and GFP expression. Shown in Figure 5F is a representative image of a WT stage 3 neuron next to a GFP+ stage 1 mmvvee neuron. We observed 70% of GFP− WT neurons in stage 3 after 48 hr in culture. In contrast, only 10% of GFP+ mmvvee neurons progressed to stage 3, while the majority (75%) arrested in stage 1 (Figure 5H). These percentages were nearly identical to those observed in neurons derived from control and mmvvee embryos (Figure 5G) and demonstrated that the neuritogenesis defect was cell-autonomous. The inability of mmvvee neurons to form neurites in vitro was consistent with the reduced Tau-1 staining in the SVZ of mmvvee cortices, where axon development is thought to initiate (Kriegstein and Noctor, 2004; Noctor et al., 2004). We concluded that the fiber tract defect in mmvvee cortices results from an inherent block in neuritogenesis. While the actin cytoskeleton has been implicated in neurite initiation (Chuang et al., 2005), to our knowledge this study is the first to suggest a direct role for actin regulatory proteins in neuritogenesis.

Loss of Filopodia Precedes Defects in Neurite Formation

To analyze the role of Ena/VASP in neurite initiation in greater detail, we collected time-lapse movies of dissociated cortical neurons from chimeric embryos, thereby permitting analysis of matched WT and mmvvee neurons isolated from the same embryo. Over 44 hr in culture, WT
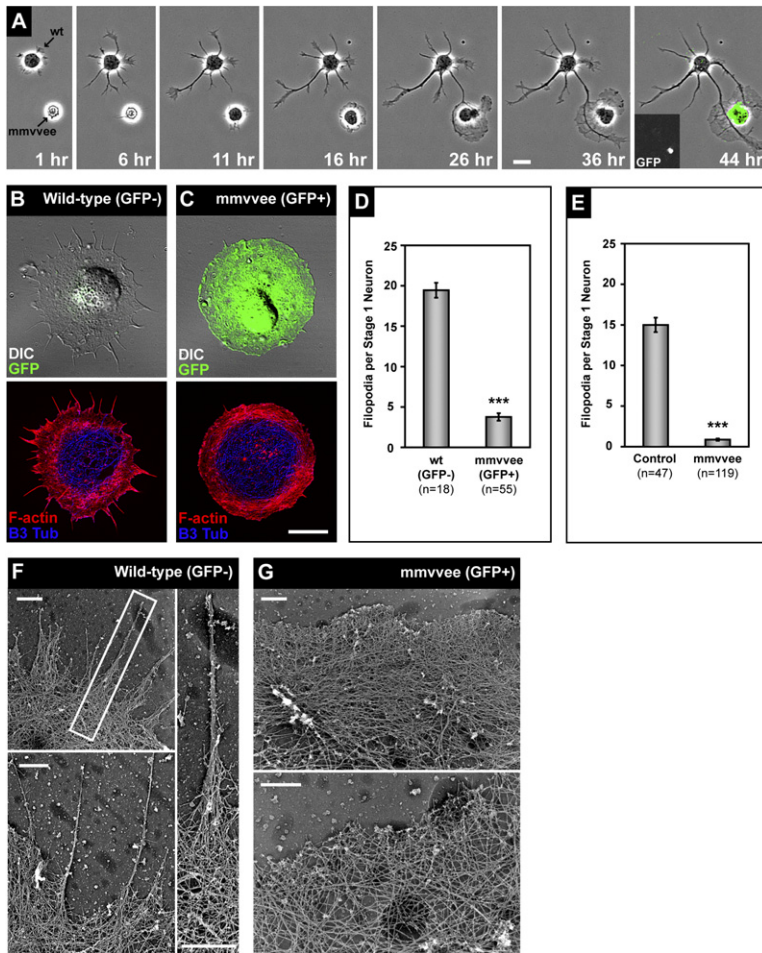
Figure 6. Ena/VASP Is Required for Actin Bundle and Filopodia Formation in Stage 1 Cortical Neurons

(A) Time-lapse phase microscopy of two dissociated cortical neurons from a single chimeric brain. The wild-type (WT) neuron differentiated from stage 1 to stage 3 within 16 hr while the mmvvee neuron remained in stage 1 after 44 hr. The final frame of the phase contrast time-lapse was overlaid with GFP signal confirming that the neuron that did not elaborate neurites was GFP+ (mmvvee).

(B and C) Two stage 1 cortical neurons from a single chimeric brain. Upper panels are a DIC and GFP overlay showing a GFP– WT neuron (B) and a GFP+ mmvvee neuron (C). The bottom two panels show the cells in the upper panels stained for β3-tubulin and F-actin. WT and mmvvee stage 1 neurons contained approximately equal amounts of F-actin. However, WT neurons (B) had many actin bundles that protruded from the cell edge as filopodia (white arrow, bottom left panel), while mmvvee neurons (C) lacked actin bundles and instead displayed prominent circumferential actin arcs within the F-actin-rich region (white arrow, bottom right panel).

(D) Bar graph showing the marked decrease in filopodia in stage 1 neurons from a single chimeric brain after 48 hr in culture (***p < 0.001, two-tailed unpaired t test with Welch's correction). Numbers under graphs in (C) and (D) indicate number of neurons examined.

(E) Bar graph showing a similar decrease in filopodia number from stage 1 neurons after 48 hr in culture from control and mmvvee littermates (***p < 0.001, two-tailed unpaired t test with Welch's correction).

(F and G) Platinum replica electron microscopy of GFP– WT (F) and GFP+ mmvvee (G) stage 1 neurons isolated from a chimeric brain. In WT neurons (F), actin filaments bundled together from both sides of the base of the filopodium. In contrast, mmvvee neurons (G) showed little actin bundling resulting in few filopodia and instead had a crosshatched network of actin filaments in the periphery and concentric actin arcs located more medially (white arrows, top panel).

Scale bar for (A), 10 μm; for (B) and (C), 10 μm; for (F) and (G), 1 μm. Data shown are means ± SEMs.

cortical neurons developed neurites (stage 2) from segmented lamellipodial/filopodial regions along the periphery of the cell, and one neurite eventually grew rapidly to form an axon (stage 3) (Figure 6A, top neuron). In contrast, the majority of GFP+ mmvvee neurons remained in stage 1 during this same period, failing to extend neurites (Figure 6A, bottom neuron, GFP overlay shown in 44 hr panel). GFP+ mmvvee neurons formed few filopodia over 44 hr in culture and remained strikingly lamellipodial, assuming a "fried egg" appearance (Figure 6A).

To analyze this phenotype in more detail, we focused on neurons at stage 1, just prior to neurite initiation. In contrast to controls (Figure 6B), mmvvee neurons lacked actin bundles and filopodia along the cell periphery (Figure 6C). Quantification of filopodia number from WT and mmvvee cortical neurons isolated from an individual chimeric brain revealed a marked (>5-fold) decrease in filopodia numbers in stage 1 mmvvee neurons (Figure 6D). A similar decrease was observed in neurons isolated from mmvvee mutants compared to those from control littermates (Figure 6E). Analysis of the actin cytoskeleton ultrastructure with correlative platinum replica electron microscopy showed that WT neurons formed straight filopodia comprised of actin filaments that coalesced from the cortical actin network on both sides of the filopodium (Figure 6F). In contrast, stage 1 mmvvee neuron actin filament arrays were crosshatched and lacked actin bundles (Figure 6G). These results indicated that loss of Ena/VASP disrupted actin network organization in cortical neurons, preventing filopodia formation. We speculate that an inherent defect in filopodia formation in mmvvee stage 1 cortical neurons is the underlying cause of the block in neuritogenesis.

Axon Formation Can Be Uncoupled from Neuronal Migration

Shortly after birth, cortical neurons extend migratory processes within the VZ, and neuronal migration is driven by

process extension coupled with nuclear translocation (O'Rourke et al., 1992). The relationship between migratory process formation and axon formation is unclear. We wanted to determine if Ena/VASP proteins localize to these migratory processes in vivo. Unfortunately, the cell density of the cortex precluded analysis of the subcellular localization of endogenous Mena by immunostaining. Therefore, we introduced EGFP-Mena into WT embryo cortices by in utero electroporation and examined its distribution in migrating cortical neurons. Compared to cytoplasmic mCherry, EGFP-Mena was concentrated at the extreme edge of the leading process and enriched in the trailing process (Figure 7A).

The localization of EGFP-Mena in migratory processes combined with the failure of mmvvee neurons to form neurites in vitro and axons in vivo led us to ask whether migratory process formation was perturbed in the absence of Ena/VASP proteins. To analyze migratory process formation, we examined the morphology of radially migrating GFP-expressing mmvvee neurons in chimeric cortices. We found that many mmvvee neurons were morphologically similar to GFP-expressing control neurons, possessing both a leading and trailing process (Figure 7C, compare to 7B). Thus, Ena/VASP proteins appeared to be dispensable for leading and trailing process formation in migrating cortical neurons despite their localization to these structures.

We also examined migratory process morphology in tangentially migrating neurons. A population of tangentially migrating interneurons display ventricle-directed migration during corticogenesis and can be visualized with the neuronal marker β3-tubulin (Nadarajah et al., 2002). We observed β3-tubulin+ neurons in the VZ and SVZ of both control and mmvvee brains (Figures 7D and 7E), with no apparent difference in number or organization. Higher magnification revealed that migratory process formation and morphology were similar between control (Figure 7D, inset) and mmvvee neurons (Figure 7E, inset). Taken together, our results indicated that migratory process formation, unlike neurite initiation, does not require Ena/VASP.

DISCUSSION

In this study, we uncovered essential requirements for Ena/VASP during cortical development by examining mmvvee embryos and chimeras containing Ena/VASP null cells. We found that loss of Ena/VASP causes cobblestone cortex, alters cortical positioning, and blocks neurite initiation and concomitant fiber tract formation. While Ena/VASP function in axon navigation has been well established, the critical role for Ena/VASP in neurite initiation discovered in this study reveals an unexpected function for Ena/VASP in nervous system development. Together, our findings define critical roles for Ena/VASP during corticogenesis while offering novel insight into neuritogenesis and the relationship between neuronal migration and axon formation.

Cortical Neuritogenesis Requires Ena/VASP Function

The IZ, typically dominated by axonal fibers, was significantly reduced in thickness in mmvvee cortices. The few axonal fibers occupying the IZ were snarled, disorganized, and immature. In vitro analysis of neuronal stage development revealed that loss of Ena/VASP caused a cell-autonomous block in neuritogenesis; such a block would prevent subsequent axon formation during cortical development. We conclude that an inherent defect in neuritogenesis abolishes fiber tract formation in mmvvee cortices.

The absence of fiber tracts in mmvvee brains and failure of mmvvee neurons to make neurites was both striking and unexpected. These phenotypes are far more severe than predicted from studies in invertebrates where loss of Ena/VASP disrupts axon guidance, but does not block axon formation (Krause et al., 2003). We suggest that this difference largely reflects the complexity of the mammalian cortex and the role Ena/VASP has evolved in cortical development. It is important to note that neurons outside the cortex in mmvvee mutants do form axons, although they are not guided properly (A.V.K. and F.B.G., unpublished data). Therefore, extracortical neurons likely possess some intrinsic factor that can compensate for loss of Ena/VASP or are exposed to some environmental cue absent from the cortex that bypasses the requirement for Ena/VASP. It is also important to note that under conditions where mmvvee extracortical neurons form neurites, neuritogenesis is always preceded by filopodia formation (E.W.D. and F.B.G., unpublished data). It is possible that invertebrates use a mechanism similar to vertebrate extracortical neurons to bypass the requirement for Ena/VASP function during neuritogenesis.

Our results also indicate that all three vertebrate Ena/VASP proteins play critical roles in neuritogenesis and axon formation, as fiber tract phenotypes were only observed with complete loss of Mena, VASP, and EVL. This is consistent with past observations showing all three vertebrate Ena/VASP proteins—Mena, VASP, and EVL—are expressed in multiple regions of the developing cortex (Goh et al., 2002; Lanier et al., 1999), notably the SVZ, IZ, and CP, areas where neurite/axon formation are believed to occur (Noctor et al., 2004).

We did observe axons in the IZ of mmvvee cortices, although they were immature and disorganized. In vitro, roughly 25% of mmvvee neurons were able to advance to stage 2 or stage 3, indicating that a small percentage of mmvvee neurons can make neurites and potentially axons. Thus, a small percentage of mutant neurons are expected to make axons in vivo. The few axons observed in the IZ could arise from these "escapers" and be cortical in origin; alternatively, they may represent thalamic axons. Regardless, it is clear that loss of Ena/VASP significantly reduces axon formation in the cortex, blocking IZ expansion and organization.

Cytoskeleton dynamics drive neurite formation, though signaling pathways and machinery that drive and regulate the cytoskeleton during neurite formation remain largely
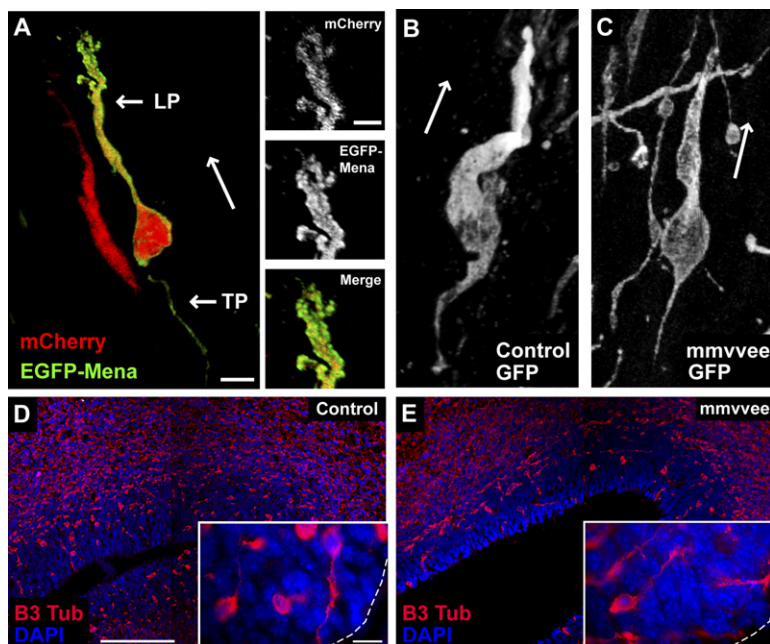
Figure 7. Migratory Process Formation Is Independent of Ena/VASP

(A) Cortical neuron expressing EGFP-Mena and mCherry migrating into the cortical plate (CP) of an E16.5 embryo. The long white arrow points in the direction of migration. EGFP-Mena localized to both leading and trailing processes (LP and TP, respectively). In particular, EGFP-Mena was enriched at the tip of the leading process (right panels).

(B and C) mmvvee neurons expressing gap-EGFP (a membrane-targeted version of EGFP) observed migrating through the CP of chimeric cortices (C) were morphologically similar to electroporated control neurons expressing gap-EGFP, possessing leading and trailing processes. White arrows point in the direction of migration.

(D and E) Coronal sections through the cortices of E16.5 control (D) and mmvvee (E) littermates were labeled with the neuronal-specific marker β3-tubulin (B3 Tub, red) and DAPI (blue). Multiple neurons, most likely tangentially migrating interneurons, were observed extending migratory processes in the ventricular zone (VZ) of both control and mmvvee brains. There was no detectable difference in the number or morphology of neurons in the VZ of control and mmvvee brains. The dashed white line in the high-magnification insets in (D) and (E) marks the border of the VZ.

Scale bar for (A), 10 μm, for insets in (A), 5 μm; for (B) and (C), 10 μm; for (D) and (E), 100 μm, for insets in (D) and (E), 10 μm.

unknown. This study is the first to demonstrate the importance of Ena/VASP in regulating this critical process in neuronal development. Mechanistically, Ena/VASP proteins regulate actin filament elongation and bundling (Bear et al., 2002) and play a pivotal role in filopodia formation in growth cones (Lebrand et al., 2004). In this report, we demonstrate that loss of Ena/VASP causes a striking reduction in actin bundle and filopodia formation in stage 1 cortical neurons. Failure to form filopodia in Ena/VASP-deficient neurons preceded the neurite initiation defect, suggesting that lack of filopodia may be the primary cause of the block in neuritogenesis. The importance of filopodia in promoting neurite formation is explored further in Dent et al. (2007).

How might filopodia formation promote neurite formation? Stage 1 neurons are decorated with dynamic actin-rich lamellipodial and filopodial extensions. While it has been postulated previously that these extensions provide the structural basis for neurite formation (da Silva and Dotti, 2002; Dehmelt and Halpain, 2004), our work directly demonstrates that loss of filopodia precedes defects in neuritogenesis. It is known that actin bundles within filopodia can serve as tracks for microtubule exploration (Schaefer et al., 2002). Microtubule binding proteins are also implicated in neurite initiation (Dehmelt and Halpain, 2004); therefore, a failure in filopodia formation could lead to a secondary defect in microtubule-dependent functions required for neuritogenesis. Thus, the function of Ena/VASP proteins as regulators of filopodia formation in stage 1 neurons suggests these molecules could control the early morphological changes in neurons required for neu-

ritogenesis. Interestingly, the necessity of Ena/VASP function in filopodia and neurite formation stands in marked contrast to its dispensability in another actin-dependent process, neuronal migration (discussed below).

A New Model for Cobblestone Cortex

We found that loss of Ena/VASP promotes ectopia formation, one of the first observations that link an actin-binding protein directly to the etiology of cobblestone cortex. Our data are consistent with a model in which defects in radial glia are a primary cause of ectopia formation in mmvvee cortices, though formal proof will require further experiments in which Ena/VASP is inactivated selectively in radial glia. Ectopia growth and spread could also be assisted by an intrinsic defect in neuronal migration that promotes invasion into the subarachnoid space. Thus, ectopia formation in mmvvee cortices may reflect the combination of a non-cell-autonomous defect in PM integrity and intrinsic defect in neuronal migration.

Though originally described as a neuronal migration disorder, a defect in neuronal migration does not appear to be the primary defect in the pathology of cobblestone cortex. Instead, both human disorders and mouse models of cobblestone cortex are usually linked to ECM proteins or molecules directly involved in cell:matrix adhesion (Beggs et al., 2003; Bielas et al., 2004; Costell et al., 1999; Georges-Labouesse et al., 1998; Graus-Porta et al., 2001; Halfter et al., 2002). Ectopias were never observed in high percentage chimeric cortices, indicating that loss of Ena/VASP from cortical neurons was not sufficient to promote ectopia formation. Similarly, no invasion into

the marginal zone in either chimeric or mmvvee (outside of ectopias) cortices was noted, indicating that when the PM was intact, neurons remained in the CP. Therefore, while an inherent defect in neuronal migration could exacerbate ectopia growth and spread in mmvvee cortices, it is unlikely to be the primary cause of ectopia formation.

Interestingly, ectopias in mmvvee cortices share some similarities to ectopias described in conditional FAK mutants (Beggs et al., 2003); most notably, the size of individual ectopias and the formation of axonal fibers descending from ectopias. Ena/VASP and FAK localize to focal adhesions and function in integrin signaling (Aszodi et al., 1999; Hauser et al., 1999; Parsons, 2003). Ectopia formation was linked to FAK deletion from radial glia and meningeal fibroblasts but not from cortical neurons, demonstrating that the primary cause of ectopia formation is a defect in PM integrity (Beggs et al., 2003). Although we did not observe a defect in laminin organization from meningeal fibroblasts, it is possible that Ena/VASP functions in glial endfeet adhesion to the PM, possibly via integrin signaling. (Aszodi et al., 1999; Hauser et al., 1999; Parsons, 2003). Alternatively, loss of Ena/VASP could disrupt endfoot:endfoot cell-cell adhesion and consequently compromise barrier integrity, a possibility consistent with earlier work indicating a role for Ena/VASP in cell-cell adhesion (Scott et al., 2006; Vasioukhin et al., 2000) and our recent observations (Furman et al., 2007). Further experiments using a glial-specific Ena/VASP deletion will be required to determine the precise defects that give rise to the formation of neuronal ectopias.

Cortical Positioning in the Absence of Ena/VASP

In chimeric cortices, Ena/VASP-deficient neurons concentrated in superficial regions of a given cortical layer or layers rather than being equally distributed across the layer or layers. This intralayer positioning phenotype is distinct from previously described defects in cortical migration (Bielas et al., 2004). Retardation of neuronal migration disrupts lamination in type-1 lissencephaly, whereas failure to recognize stop cues causes an inversion in cortical layering in reelin-signaling mutants (Gressens, 2006). Loss of Ena/VASP did not severely compromise CP formation, and migration initiation appeared unaffected. Furthermore, outside of ectopias, we found no evidence of marginal zone invasion in either mmvvee or chimeric cortices, suggesting that neurons respected classic positioning signals in the absence of Ena/VASP. This was consistent with layer boundaries being respected by mmvvee neurons in chimeras.

A previous study found that inhibition of Ena/VASP function caused aberrant targeting of early-born neurons to more superficial layers in the CP (Goh et al., 2002). That study described a more severe positioning defect than what we observed, a difference that could be attributed to variations in experimental design and stage of analysis. However, in both cases a similar trend was observed: Ena/VASP-deficient neurons targeted to more superficial regions of the cortex. Further experiments are needed to discern whether loss of Ena/VASP alters radial migration to the CP, termination of migration, or postmigratory sorting once in the CP.

It is worth noting that in cortical lamination mutants such as reeler, mispositioned neurons extend axons (Bielas et al., 2004). Thus, it is unlikely that the intralayer positioning defect caused by loss of Ena/VASP is responsible for the profound loss of fiber tracts in mmvvee cortices. In fact, our results suggest that neuritogenesis defects are independent of cortical mispositioning defects in mmvvee cortices (described below).

Migratory Process versus Axonal Process Formation

Glial-guided radially migrating neurons have a characteristic bipolar morphology: a leading process that points in the direction of migration and trailing process that follows behind. The importance of the actin cytoskeleton in cortical neuron leading process function is largely unknown, though evidence from other neuronal cell types suggests actin assembly is critical for leading process motility (Rivas and Hatten, 1995). When expressed in cortical neurons, EGFP-Mena was highly enriched at the tip of the leading process. However, we found that leading process formation and morphology was unaffected by loss of Ena/VASP. We suggest that Ena/VASP proteins—similar to their role in other systems—could regulate leading process dynamics and/or adhesion; in fact, the observed Ena/VASP-dependent intralayer positioning defects could reflect a defect in leading process function during radial migration. Future work is needed to elucidate the role of the Ena/VASP proteins and the importance of the actin cytoskeleton in leading process formation and function.

Most migrating neurons send out a trailing process, and it has been suggested that the trailing process becomes an axon (Noctor et al., 2004; Tsai et al., 2005). Interestingly, radially migrating neurons do not proceed directly to the CP after genesis in the VZ; instead, they proceed through a series of stages, at one point arresting in the SVZ. During this SVZ arrest, neurons enter a multipolar state whereupon they send out multiple processes. Eventually, neurons extend a single migratory process toward the ventricular surface. Locomotion resumes after neurons acquire a bipolar morphology by extending another leading process in the direction of the PM. This ventricle-contacting process is retained by most neurons; that is, what was once the leading process becomes the trailing process and the putative developing axon (Noctor et al., 2004). Unfortunately, the high percentage of labeled cells in the cortex of chimeric embryos prevented us from determining if GFP+ mmvvee cells formed these ventricle-contacting processes. However, we observed mmvvee neurons with trailing processes during later stages of migration and did not detect a defect in neuronal entry into the CP, suggesting that mmvvee neurons were able to progress through all phases of radial migration.

If the trailing process develops into an axon, how do we reconcile this with our observations that loss of Ena/VASP

blocks axon fiber tract formation in vivo and inhibits neurite formation in vitro? It is possible that this trailing process, a former migratory process, is formed in mmvvee neurons since there appears to be no defect in migratory process formation in the absence of Ena/VASP. However, without Ena/VASP proteins, this process might fail to develop significantly by growing tangentially within the VZ/SVZ as observed in WT neurons (Noctor et al., 2004). In fact, we observed a marked decrease in Tau-1+ fibers in the SVZ of mmvvee cortices, consistent with this idea. Alternatively, nascent axons may develop independently from the cell body and grow along the trailing process; there is no direct high-resolution evidence demonstrating conclusively that the trailing process itself actually develops into an axon (Noctor et al., 2004; Tsai et al., 2005). Finally, a large percentage (roughly 40%) of radially migrating neurons do not extend a migratory process toward the ventricular surface (Noctor et al., 2004), suggesting that axon formation occurs by other means. Ena/VASP proteins might be critical for these neurons to form neurites independent of the trailing process, though given the severity of the phenotype in mmvvee cortices, we suggest additional defects (explained above) are also likely.

In conclusion, we have identified an in vivo model for analysis of neurite initiation. The results presented here identify Ena/VASP proteins as key factors in the earliest steps of neurite initiation and define their requirement for axon formation in the developing cortex. Our findings also underscore the role of filopodia and the actin cytoskeleton in the initial stages of neuritogenesis and concomitant axon formation.

EXPERIMENTAL PROCEDURES

Generation of EVL Knockout Mice

A BAC containing the EVL locus (GeneID:14026) was obtained from Genome Systems. The targeting vector was constructed by subcloning a 1.0 kb genomic DNA fragment upstream of EVL exon 2 and a 5.0 kb fragment downstream of exon 3 into vector pPGKneobpA-lox2PGKDTA (a gift from Philippe Soriano). The targeting vector was electroporated into R1 ES cells. Over 1000 G418-resistant ES colonies were picked and screened for homologous recombination by PCR. Five clones were identified, and homologous recombination reconfirmed by Southern blot. Four of the five clones produced high percentage chimeras, but subsequent breeding revealed only one germline clone—the EVL knockout line used in this study.

Mouse Colony

All animal work was approved by the MIT Committee on Animal Care. Chimeric mice were initially crossed to C57/B6 mice to determine germline transmission of the mutated EVL allele. All experiments described were conducted with mutant mice on a mixed background, primarily a mix of Balb/c and 129/Sv.

For timed pregnancies, mating pairs were set up in the evening and checked for vaginal plugs the following morning; day of plug was deemed embryonic stage E0.5. Plugged females were removed from the mating pair and sacrificed at the appropriate time.

Generation of WT/mmvvee Chimeras

To facilitate the isolation of ES cells lacking all Ena/VASP proteins, a conditional allele of EVL was constructed, denoted as E^c. E^c was created by flanking exon 2 of EVL with LoxP sites (for further details regarding construction, please contact the corresponding author). The E^c allele did not disrupt EVL expression, but exposure to Cre recombinase deleted exon 2 and abolished EVL expression (data not shown). MmvvE^{c}E^c × MmvvE^{c}E^c timed pregnancies produced mmvvE^{c}E^c blastocysts, from which ES cell lines were established. A Cre-expression plasmid was transfected into mutant lines, individual colonies picked, expanded, and genotyped for recombination at the E^c locus. Only clones in which both E^c alleles had recombined were expanded (now functionally mmvvee). These ES clones were infected with either pLL4.4, a lentivirus expressing EGFP under control of the CAG promoter, or pLL4.4 gap-EGFP, a membrane-targeted version of EGFP. Infections were conducted as previously described (Rubinson et al., 2003). GFP+ colonies were picked, expanded, and injected into WT B6 blastocysts to generate chimeric embryos. Chimeric embryos were harvested at various embryonic stages (E14.5–E18.5), scored for GFP expression under a dissection microscope outfitted with fluorescence, and prepped for frozen or vibratome sectioning or cortical cell culture.

In Utero Electroporation

Electroporations were performed on timed pregnant Swiss-Webster mice at E12.5 as previously described (Shu et al., 2004). One microliter of DNA solution containing either a 1:1 ratio of pCAX-EGFP-Mena and pCAX-mCherrry or pLL4.4R gap-EGFP was injected into the lateral ventricle of embryos through the uterine wall, and electrical pulses were applied (five repeats of 30 V for 50 ms with an interval of 950 ms). Two to four days after electroporation, embryos were dissected, perfused with 4% paraformaldehyde, and prepared for sectioning.

Antibodies

Western: EVL (1404, 1:5000), Mena (monoclonal, 1:100 for western), VASP (2010, 1:5000). IHC: NF (2H3, DSHB, 1:200), TAG-1 (DSHB, 1:50-1:100), β3-tubulin (Promega, 1:1000-1:5000), Laminin (Abcam, 1:200-1:500), Nestin (DSHB, 1:100; Molecular Probes, 1:1000), Tau-1 (Chemicon, 1:200), GFP (Molecular Probes, 1:250-1:1000), Tbr1 (gift from Morgan Sheng, 1:100), Foxp1 (gift from Edward Morrisey, 1:500).

Histology and Immunohistochemistry

Bouin's fixed tissues were embedded in paraffin, sectioned, and stained with H&E using standard techniques. Tissues for frozen sectioning were fixed lightly in 4% PFA on ice for 1 hr, washed three times in cold PBS, soaked in 30% sucrose in PBS overnight at 4°C, embedded in OCT compound (Tissue Tek), and stored at −80°C until sectioned. For IHC, 10 micron cryostat sections were dipped in ice-cold acetone for 2 min, air-dried for 15 min, rinsed twice in PBS, and blocked in PBS plus 10% normal goat or donkey serum, 5% BSA, and 0.05% Tween. Blocking was performed overnight at 4°C or for 1–2 hr at room temperature. Sections were incubated with primary and secondary antibodies diluted in PBS plus 1% normal serum, 1% BSA, and 0.05% Tween either overnight at 4°C or for 1 hr at room temperature. Slides were washed three times in PBS with gentle agitation after each antibody incubation. DAPI staining was performed after secondary incubation. After staining, all slides were mounted in Fluoromount-G (Electron Microscopy Sciences) and imaged.

MRI and μDTI

Before imaging, Bouin's-fixed embryos were washed in PBS for more than 24 hr to remove the fixation solution and transferred into homebuilt MR-compatible tubes. The tubes were then filled with fomblin (Fomblin Profludropolyether, Ausimont, Thorofare, New Jersey, USA) to prevent dehydration. MRI and μDTI were performed as previously described (Zhang et al., 2005; Mori and Zhang, 2006).

Meningeal Fibroblast Culture and Laminin Production

Meningeal fibroblasts were isolated from E14.5 mutant embryos and cultured as previously described (Beggs et al., 2003). To examine

laminin production and organization, control and mmvvee fibroblasts were plated onto acid-washed glass coverslips coated with poly-D-lysine (1 mg/ml), cultured for 3 days, fixed in 4% PFA, and stained for laminin.

Cortical Cell Culture

Primary dissociated cortical neurons were prepared from E14.5 mice and cultured in serum-free medium essentially as described (Lebrand et al., 2004). Neurons were initially cultured in 5% fetal bovine serum (FBS) (Hyclone) in Neurobasal Medium (GIBCO) with B27 supplements and glutamine, and later switched to serum-free medium after 1 hr in culture. Neurons were plated on coverslips coated with 1.0 mg/ml poly-d-lysine (PdL) (Sigma) at a concentration of 5000 cells/cm^2. Neurons were fixed in warmed 4% paraformaldehyde/0.25% gluteraldehyde in Krebs' solution with 0.4 M sucrose (Lebrand et al., 2004) to preserve the cytoskeleton. Cells were blocked in 10% BSA/PBS and extracted with 0.2% Triton X-100 in block prior to staining.

Imaging

Tissue immunostaining was imaged on either a Deltavision Spectris deconvolution system (Applied Precision) or Nikon TE2000 microscope outfitted with a spinning disk confocal head (Yokagawa). Z series were collected on the Deltavision, and when applicable, deconvolved using softWoRx (Applied Precision). In some instances, panels of Z series were collected and stitched together in softWoRx to form larger images.

Supplemental Data

The Supplemental Data for this article can be found online at http://www.neuron.org/cgi/content/full/56/3/441/DC1/.

REFERENCES

Adler, C.E., Fetter, R.D., and Bargmann, C.I. (2006). UNC-6/Netrin induces neuronal asymmetry and defines the site of axon formation. Nat. Neurosci. 9, 511–518.

Applewhite, D.A., Barzik, M., Kojima, S.I., Svitkina, T.M., Gertler, F.B., and Borisy, G.G. (2007). Ena/VASP proteins have an anti-capping independent function in filopodia formation. Mol. Biol. Cell 18, 2579–2591.

Aszodi, A., Pfeifer, A., Ahmad, M., Glauner, M., Zhou, X.H., Ny, L., Andersson, K.E., Kehrel, B., Offermanns, S., and Fässler, R. (1999). The

vasodilator-stimulated phosphoprotein (VASP) is involved in cGMP- and cAMP-mediated inhibition of agonist-induced platelet aggregation, but is dispensable for smooth muscle function. EMBO J. 18, 37–48.

Bear, J.E., Svitkina, T.M., Krause, M., Schafer, D.A., Loureiro, J.J., Strasser, G.A., Maly, I.V., Chaga, O.Y., Cooper, J.A., Borisy, G.G., and Gertler, F.B. (2002). Antagonism between Ena/VASP proteins and actin filament capping regulates fibroblast motility. Cell 109, 509–521.

Beggs, H.E., Schahin-Reed, D., Zang, K., Goebbels, S., Nave, K.A., Gorski, J., Jones, K.R., Sretavan, D., and Reichardt, L.F. (2003). FAK deficiency in cells contributing to the basal lamina results in cortical abnormalities resembling congenital muscular dystrophies. Neuron 40, 501–514.

Bielas, S., Higginbotham, H., Koizumi, H., Tanaka, T., and Gleeson, J.G. (2004). Cortical neuronal migration mutants suggest separate but intersecting pathways. Annu. Rev. Cell Dev. Biol. 20, 593–618.

Chuang, J.Z., Yeh, T.Y., Bollati, F., Conde, C., Canavosio, F., Caceres, A., and Sung, C.H. (2005). The dynein light chain Tctex-1 has a dynein-independent role in actin remodeling during neurite outgrowth. Dev. Cell 9, 75–86.

Costell, M., Gustafsson, E., Aszodi, A., Morgelin, M., Bloch, W., Hunziker, E., Addicks, K., Timpl, R., and Fässler, R. (1999). Perlecan maintains the integrity of cartilage and some basement membranes. J. Cell Biol. 147, 1109–1122.

da Silva, J.S., and Dotti, C.G. (2002). Breaking the neuronal sphere: regulation of the actin cytoskeleton in neuritogenesis. Nat. Rev. Neurosci. 3, 694–704.

de Lima, A.D., Merten, M.D., and Voigt, T. (1997). Neuritic differentiation and synaptogenesis in serum-free neuronal cultures of the rat cerebral cortex. J. Comp. Neurol. 382, 230–246.

Dehmelt, L., and Halpain, S. (2004). Actin and microtubules in neurite initiation: are MAPs the missing link? J. Neurobiol. 58, 18–33.

Dent, E.W., Kwiatkowski, A.V., Mebane, L.M., Philippar, U., Barzik, M., Rubinson, D.A., Gupton, S., van Veen, J.E., Furman, C., Zhang, J., et al. (2007). Filipodia are required for cortical neurite initiation. Nat. Cell Biol., in press.

Dwivedy, A., Gertler, F.B., Miller, J., Holt, C.E., and Lebrand, C. (2007). Ena/VASP function in retinal axons is required for terminal arborization but not pathway navigation. Development 134, 2137–2146.

Elder, G.A., Friedrich, V.L., Jr., Bosco, P., Kang, C., Gourov, A., Tu, P.H., Lee, V.M., and Lazzarini, R.A. (1998). Absence of the mid-sized neurofilament subunit decreases axonal calibers, levels of light neurofilament (NF-L), and neurofilament content. J. Cell Biol. 141, 727–739.

Ferland, R.J., Cherry, T.J., Preware, P.O., Morrisey, E.E., and Walsh, C.A. (2003). Characterization of Foxp2 and Foxp1 mRNA and protein in the developing and mature brain. J. Comp. Neurol. 460, 266–279.

Friede, R.L., and Samorajski, T. (1970). Axon caliber related to neurofilaments and microtubules in sciatic nerve fibers of rats and mice. Anat. Rec. 167, 379–387.

Furman, C., Sieminski, A.L., Kwiatkowski, A.V., Rubinson, D.A., Vasile, E., Bronson, R.T., Fässler, R., and Gertler, F.B. (2007). Ena/VASP is required for endothelial barrier function in vivo. J. Cell Biol., in press.

Georges-Labouesse, E., Mark, M., Messaddeq, N., and Gansmuller, A. (1998). Essential role of alpha 6 integrins in cortical and retinal lamination. Curr. Biol. 8, 983–986.

Gertler, F.B., Niebuhr, K., Reinhard, M., Wehland, J., and Soriano, P. (1996). Mena, a relative of VASP and Drosophila Enabled, is implicated in the control of microfilament dynamics. Cell 87, 227–239.

Goh, K.L., Cai, L., Cepko, C.L., and Gertler, F.B. (2002). Ena/VASP proteins regulate cortical neuronal positioning. Curr. Biol. *12*, 565–569.

Graus-Porta, D., Blaess, S., Senften, M., Littlewood-Evans, A., Damsky, C., Huang, Z., Orban, P., Klein, R., Schittny, J.C., and Muller, U. (2001). Beta1-class integrins regulate the development of laminae and folia in the cerebral and cerebellar cortex. Neuron *31*, 367–379.

Gressens, P. (2006). Pathogenesis of migration disorders. Curr. Opin. Neurol. *19*, 135–140.

Halfter, W., Dong, S., Yip, Y.P., Willem, M., and Mayer, U. (2002). A critical function of the pial basement membrane in cortical histogenesis. J. Neurosci. *22*, 6029–6040.

Han, Y.H., Chung, C.Y., Wessels, D., Stephens, S., Titus, M.A., Soll, D.R., and Firtel, R.A. (2002). Requirement of a vasodilator-stimulated phosphoprotein family member for cell adhesion, the formation of filopodia, and chemotaxis in dictyostelium. J. Biol. Chem. *277*, 49877–49887.

Hand, R., Bortone, D., Mattar, P., Nguyen, L., Heng, J.I., Guerrier, S., Boutt, E., Peters, E., Barnes, A.P., Parras, C., et al. (2005). Phosphorylation of Neurogenin2 specifies the migration properties and the dendritic morphology of pyramidal neurons in the neocortex. Neuron *48*, 45–62.

Hatten, M.E. (2002). New directions in neuronal migration. Science *297*, 1660–1663.

Hauser, W., Knobeloch, K.P., Eigenthaler, M., Gambaryan, S., Krenn, V., Geiger, J., Glazova, M., Rohde, E., Horak, I., Walter, U., and Zimmer, M. (1999). Megakaryocyte hyperplasia and enhanced agonist-induced platelet activation in vasodilator-stimulated phosphoprotein knockout mice. Proc. Natl. Acad. Sci. USA *96*, 8120–8125.

Hevner, R.F., Shi, L., Justice, N., Hsueh, Y., Sheng, M., Smiga, S., Bulfone, A., Goffinet, A.M., Campagnoni, A.T., and Rubenstein, J.L. (2001). Tbr1 regulates differentiation of the preplate and layer 6. Neuron *29*, 353–366.

Krause, M., Dent, E.W., Bear, J.E., Loureiro, J.J., and Gertler, F.B. (2003). Ena/VASP proteins: regulators of the actin cytoskeleton and cell migration. Annu. Rev. Cell Dev. Biol. *19*, 541–564.

Kriegstein, A.R., and Noctor, S.C. (2004). Patterns of neuronal migration in the embryonic cortex. Trends Neurosci. *27*, 392–399.

Lambert de Rouvroit, C., and Goffinet, A.M. (2001). Neuronal migration. Mech. Dev. *105*, 47–56.

Lanier, L.M., Gates, M.A., Witke, W., Menzies, A.S., Wehman, A.M., Macklis, J.D., Kwiatkowski, D., Soriano, P., and Gertler, F.B. (1999). Mena is required for neurulation and commissure formation. Neuron *22*, 313–325.

Lebrand, C., Dent, E.W., Strasser, G.A., Lanier, L.M., Krause, M., Svitkina, T.M., Borisy, G.G., and Gertler, F.B. (2004). Critical role of Ena/VASP proteins for filopodia formation in neurons and in function downstream of netrin-1. Neuron *42*, 37–49.

Loureiro, J.J., Rubinson, D.A., Bear, J.E., Baltus, G.A., Kwiatkowski, A.V., and Gertler, F.B. (2002). Critical roles of phosphorylation and actin binding motifs, but not the central proline-rich region, for Ena/vasodilator-stimulated phosphoprotein (VASP) function during cell migration. Mol. Biol. Cell *13*, 2533–2546.

Luo, L. (2002). Actin cytoskeleton regulation in neuronal morphogenesis and structural plasticity. Annu. Rev. Cell Dev. Biol. *18*, 601–635.

Marin, O., and Rubenstein, J.L. (2003). Cell migration in the forebrain. Annu. Rev. Neurosci. *26*, 441–483.

Mejillano, M.R., Kojima, S., Applewhite, D.A., Gertler, F.B., Svitkina, T.M., and Borisy, G.G. (2004). Lamellipodial versus filopodial mode of the actin nanomachinery: pivotal role of the filament barbed end. Cell *118*, 363–373.

Menzies, A.S., Aszodi, A., Williams, S.E., Pfeifer, A., Wehman, A.M., Goh, K.L., Mason, C.A., Fässler, R., and Gertler, F.B. (2004). Mena and vasodilator-stimulated phosphoprotein are required for multiple actin-dependent processes that shape the vertebrate nervous system. J. Neurosci. *24*, 8029–8038.

Miner, J.H., and Yurchenco, P.D. (2004). Laminin functions in tissue morphogenesis. Annu. Rev. Cell Dev. Biol. *20*, 255–284.

Mori, S., and Zhang, J. (2006). Principles of diffusion tensor imaging and its applications to basic neuroscience research. Neuron *51*, 527–539.

Nadarajah, B., Alifragis, P., Wong, R.O., and Parnavelas, J.G. (2002). Ventricle-directed migration in the developing cerebral cortex. Nat. Neurosci. *5*, 218–224.

Niewmierzycka, A., Mills, J., St-Arnaud, R., Dedhar, S., and Reichardt, L.F. (2005). Integrin-linked kinase deletion from mouse cortex results in cortical lamination defects resembling cobblestone lissencephaly. J. Neurosci. *25*, 7022–7031.

Noctor, S.C., Martinez-Cerdeno, V., Ivic, L., and Kriegstein, A.R. (2004). Cortical neurons arise in symmetric and asymmetric division zones and migrate through specific phases. Nat. Neurosci. *7*, 136–144.

O'Rourke, N.A., Dailey, M.E., Smith, S.J., and McConnell, S.K. (1992). Diverse migratory pathways in the developing cerebral cortex. Science *258*, 299–302.

Olson, E.C., and Walsh, C.A. (2002). Smooth, rough and upside-down neocortical development. Curr. Opin. Genet. Dev. *12*, 320–327.

Olson, E.C., Kim, S., and Walsh, C.A. (2006). Impaired neuronal positioning and dendritogenesis in the neocortex after cell-autonomous Dab1 suppression. J. Neurosci. *26*, 1767–1775.

Parsons, J.T. (2003). Focal adhesion kinase: the first ten years. J. Cell Sci. *116*, 1409–1416.

Rivas, R.J., and Hatten, M.E. (1995). Motility and cytoskeletal organization of migrating cerebellar granule neurons. J. Neurosci. *15*, 981–989.

Rubinson, D.A., Dillon, C.P., Kwiatkowski, A.V., Sievers, C., Yang, L., Kopinja, J., Rooney, D.L., Ihrig, M.M., McManus, M.T., Gertler, F.B., et al. (2003). A lentivirus-based system to functionally silence genes in primary mammalian cells, stem cells and transgenic mice by RNA interference. Nat. Genet. *33*, 401–406.

Schaefer, A.W., Kabir, N., and Forscher, P. (2002). Filopodia and actin arcs guide the assembly and transport of two populations of microtubules with unique dynamic parameters in neuronal growth cones. J. Cell Biol. *158*, 139–152.

Schirenbeck, A., Arasada, R., Bretschneider, T., Stradal, T.E., Schleicher, M., and Faix, J. (2006). The bundling activity of vasodilator-stimulated phosphoprotein is required for filopodium formation. Proc. Natl. Acad. Sci. USA *103*, 7694–7699.

Scott, J.A., Shewan, A.M., den Elzen, N.R., Loureiro, J.J., Gertler, F.B., and Yap, A.S. (2006). Ena/VASP proteins can regulate distinct modes of actin organization at cadherin-adhesive contacts. Mol. Biol. Cell *17*, 1085–1095.

Shu, T., Ayala, R., Nguyen, M.D., Xie, Z., Gleeson, J.G., and Tsai, L.H. (2004). Ndel1 operates in a common pathway with LIS1 and cytoplasmic dynein to regulate cortical neuronal positioning. Neuron *44*, 263–277.

Sievers, J., Pehlemann, F.W., Gude, S., and Berry, M. (1994). Meningeal cells organize the superficial glia limitans of the cerebellum and produce components of both the interstitial matrix and the basement membrane. J. Neurocytol. *23*, 135–149.

Song, H., and Poo, M. (2001). The cell biology of neuronal navigation. Nat. Cell Biol. *3*, E81–E88.

Sur, M., and Rubenstein, J.L. (2005). Patterning and plasticity of the cerebral cortex. Science *310*, 805–810.

Tsai, J.W., Chen, Y., Kriegstein, A.R., and Vallee, R.B. (2005). LIS1 RNA interference blocks neural stem cell division, morphogenesis, and motility at multiple stages. J. Cell Biol. *170*, 935–945.

Vasioukhin, V., Bauer, C., Yin, M., and Fuchs, E. (2000). Directed actin polymerization is the driving force for epithelial cell-cell adhesion. Cell *100*, 209–219.

Yee, K.T., Simon, H.H., Tessier-Lavigne, M., and O'Leary, D.M. (1999). Extension of long leading processes and neuronal migration in the mammalian brain directed by the chemoattractant netrin-1. Neuron *24*, 607–622.

Zhang, J., Miller, M.I., Plachez, C., Richards, L.J., Yarowsky, P., van Zijl, P., and Mori, S. (2005). Mapping postnatal mouse brain development with diffusion tensor microimaging. Neuroimage *26*, 1042–1051.